

HF CHEMICAL LASER ANALYSIS OF TWIN PLANE JETS VIA A KINETIC THEORY APPROACH

Shu-Hao Chuang and Zuu-Chang Hong*

Institute of Mechanical Engineering, National Chung-Hsing University, Taichung, Taiwan 40227, Republic of China and

**Department of Mechanical Engineering, National Central University, Chungli, Taiwan 32054, Republic of China*

ABSTRACT

Solutions of the twin plane jets HF chemical laser flow based on a turbulent kinetic theory, due to a modified Green's function method, are presented. The calculated results of probability density function (PDF) of various chemical species in velocity space, and mass fraction concentration distributions of various reactants and products in the flow field, are revealed and discussed in this analysis. The transport phenomena of different pumping rate, collisional deactivation rate, and radiative deactivation rate in the interaction between the twin plane jets HF chemical laser show that the properties of species mass fraction concentrations, collisional reaction rate, and radiative incident intensity are the dominant factors. The present study provides the fundamentals for theoretical understanding of twin plane jets HF chemical laser and further application to multiple-jet HF chemical laser analysis.

KEY WORDS Turbulent kinetic theory Twin plane jets HF chemical laser PDF

NOMENCLATURE

C_i	mass fraction of species i	\tilde{S}	S/D
D	width of jet	t	time
E	turbulent energy	\bar{U}_j	jet stream velocity
E_{0i}	source condition of turbulent energy	\bar{U}_M	jet velocity of mixing centre
$E_{v,j}$	rotation-vibration energy	\bar{U}_0	$\bar{U}_M - \bar{U}_\infty$
F	probability density function (PDF) of C	\bar{U}_∞	surrounding velocity
f	probability density function of fluid element	u, v, w	instantaneous velocity in the x , y , and z directions, respectively
G	Green's function	u_j	tensor velocity
$G_{v,j}$	integrated gain	$\bar{u}, \bar{v}, \bar{w}$	average velocity in the x , y , and z directions, respectively
h	Planck constant	u', v', w'	fluctuation velocity in the x , y , and z directions, respectively
$I_{v,j}^i$	radiative incident intensity	x_c	lasing optical cavity length
$I_{v,j}^o$	radiative output intensity	x_j	tensor coordinate
J	rotational quantum number	β	$\beta_1 + \beta^v$
K_b	Boltzmann constant	β_1	characteristics relaxation rate of the energy-containing eddies
K_{pm}	pumping reaction rate	β^v	characteristic relaxation rate of the microscale
\bar{M}	molecular weight	Γ_v	Damkohler number, $\rho K_{22} \Delta x / (\bar{M}_e u)$
N_A	Avagadro's number	Γ_t	Damkohler number, $\rho K_{a2} \Delta x / (\bar{M}_e u)$
P_{wr}	laser output power	η	chemical efficiency
Q	rotational partition function		
R	velocity ratio, $\bar{U}_\infty / \bar{U}_j$		
S	distance of central lines between twin jets		

ν	radiative frequency	d	N_2
ω	chemical reaction term	e	HF(0)
$\omega_{ch}(\nu)$	instantaneous production rate of HF at ν level for chemical reaction	f	HF(1)
$\omega_{rad}(\nu)$	instantaneous production rate of HF at ν level for radiative reaction	g	HF(2)
ρ	fluid density	h	HF(3)
		j	jet stream
		pm	pumping reaction
		νj	denotes P branch transition time ($\nu + 1, j - 1$) to (ν, j)
		$\nu\nu$	vibration-vibration collisional deactivation
<i>Subscripts and superscripts</i>		$-$ or $\langle \rangle$	ensemble average
a	F	\rightarrow	vector
av	vibration-translation collisional deactivation	i	incident
b	H_2	o	output or source condition
c	H	*	excited HF

INTRODUCTION

Analysis of chemical laser is very useful because of its wide application to engineering problems, such as the laser tube in the measurement systems of wind tunnel. Studies of twin plane jets will provide some basic understanding in the turbulent mixing, combustion and chemical laser structure of multiple jets. Solutions of twin plane jets turbulent mixing and combustion analysis^{1,2} and multiple plane jets turbulent mixing and combustion^{3,4}, based upon a kinetic theory of turbulence, were obtained. The internal physical structure of the turbulent mixing mechanisms seems better understood via the kinetic theory approach. The intention of this paper is further to solve the chemical laser of twin plane jets via a turbulent kinetic theory approach.

Population inversion of chemical laser comes from the release energy of pumping reaction. Therefore, chemical laser is also one kind of the turbulent reacting flows. According to the previous studies¹⁻⁴, the turbulent kinetic theory⁵⁻⁶, approach due to a modified Green's function method¹⁻⁴ are further extended to analyse HF chemical laser properties of the twin plane jets. Chemical laser flow which mainly utilizes the heat energy of pumping reaction to generate population inversion and lasing action, was originally suggested by Polanyi⁷. The molecular chemical laser exploits chemical reaction that results in the appearance of reacting energy of vibration excitation. The concept was not, however, demonstrated by Kasper and Pimental⁸ in 1965. Early works on this problem of the chemical laser were directed to the pulsed mode^{8,9} because of the fact that the mixing rate was slower than the chemical reaction rate. A continuously operating chemical laser flow was produced by the improvement of mixing rate of reactants¹⁰. The performance of HF chemical laser analysis was shown in References 11-13. Previous investigated works of chemical laser were focused on laser systems, in which the lasing gases are stagnant¹⁴ or dynamic¹⁵ laminar chemical laser. The internal physical structure of the laminar chemical laser mechanism seems better understood via the above investigations, but the most of multiple plane jets are the turbulent flow. The turbulent chemical laser is different from the laminar chemical laser, e.g. more homogeneous mixing occurs under the turbulent flow, but the power output and efficiency increases uncertainly in a turbulent chemical laser¹⁶. The mixing rate becomes mainly a dominant factor of the chemical reaction because the latter is limited by the former under the fast chemical reaction rate.

The net amplification property of chemical laser flow is affected by the interaction between chemical kinetics and turbulent intensity, e.g. among the pumping reaction, turbulent intensity and turbulent fluctuation. Therefore, the turbulent intensity can directly influence the chemical laser properties. The chemical lasing reaction under the premixed mixing of reactants was assumed

by Kerber *et al.*¹⁷. In practice, the mixing of chemical lasers flow are preceded under an optical cavity. Broadwell¹⁸ has assumed that both hydrogen and fluorine are immediately in homogeneous distributions in mixing region, when they enter the mixing region, and the chemical reaction occurs simultaneously. In fact, the chemical lasing reaction is a molecular-wise process; the turbulent momentum mixing is presented by eddy viscosity and averaged velocity gradient (neglected the fluctuation correlations) that is derived by the mistake results⁵. Conventional treatments for the turbulent chemical lasers with turbulent correlations were frequently replaced by the average gradient type and that the neglected characteristics of turbulent correlations would easily lead to the error results as laminar flow. Hong and Chen¹⁹ has analysed the HF chemical laser properties in a single turbulent plane jet based upon a kinetic theory of turbulence and the modified Green's function. The internal structure of chemical laser flow mechanism seems better understood via a kinetic theory approach²⁰. In order to further study the chemical laser of multiple plane jets, the intention here is to analyse the HF chemical laser of twin plane jets via a turbulent kinetic theory approach.

THEORETICAL MODEL

The derivation of the governing equations for f and F_l can be found in Reference 16, here only the presented results are as follows:

$$\frac{\partial f}{\partial t} + u_j \frac{\partial f}{\partial x_j} = \beta \frac{\partial}{\partial u_j} [(u_j - \langle u_j \rangle) f] + \frac{\beta_1}{3} E \frac{\partial^2 f}{\partial u_j \partial u_j} \quad (1)$$

$$\frac{\partial F_l}{\partial t} + u_j \frac{\partial F_l}{\partial x_j} = \beta \frac{\partial}{\partial u_j} [(u_j - \langle u_j \rangle) F_l] + \frac{\beta_1}{3} E \frac{\partial^2 F_l}{\partial u_j \partial u_j} + \omega_l f \quad (2)$$

Numerical solutions for the probability density function (PDF) in velocity space of the twin and multiple jets, turbulent mixing and combustion had been presented¹⁻⁴. Now, the above results can be used continuously to analyse the chemical laser flow. For the present problem, the geometry of turbulent twin plane jets flow is shown in *Figure 1*. It consists of two jet streams of fuel (H_2), and an oxidant (fluorine atoms) and an inert diluent. Hong²⁰ obtained the Green's function of (1) as:

$$G(x, \vec{u}, t/\vec{x}_0, \vec{u}_0, t_0) = \frac{e^{3\beta t}}{8\pi^3(AC - B^2)^{3/2}} \cdot \exp \left[- \left[C \left[\left(\vec{u} - \frac{\vec{k}}{\beta} \right) e^{\beta t} - \left(\vec{u}_0 - \frac{\vec{k}}{\beta} \right) e^{\beta t_0} \right]^2 \right. \right. \\ \left. \left. + 2B \left[\left(\vec{u} - \frac{\vec{k}}{\beta} \right) e^{\beta t} - \left(\vec{u}_0 - \frac{\vec{k}}{\beta} \right) e^{\beta t_0} \right] \cdot \left[(\vec{x} - \vec{x}_0) + \frac{\vec{u} - \vec{u}_0}{\beta} - \frac{\vec{k}}{\beta}(t - t_0) \right] \right. \right. \\ \left. \left. + A \left[(\vec{x} - \vec{x}_0) + \frac{\vec{u} - \vec{u}_0}{\beta} - \frac{\vec{k}}{\beta}(t - t_0) \right]^2 \right] / 2(AC - B^2) \right]$$

A modified Green's function method¹ was employed for the present approach. In that modified Green's function method, we assume that two turbulent streams of the same mean velocity and turbulent energy were initially separated by two infinitely long thin films (see *Figures 1* and *2*). At $t = t_0$, these thin films are suddenly removed, and the two streams begin to mix, as shown in *Figure 2a*. This instantaneous mixing phenomenon will be used to simulate the steady twin-jet mixing problem¹⁻⁴. Assume that an observer begins to move at $t = t_0$ along the x axis with velocity \vec{U}_m , as shown in *Figure 2b*. The observer will see the velocity profiles and other momentum quantities similar to those in *Figure 1* for steady-state twin jets. The simulation was justified by the experimental results with Lee and Harsha's, and Spencer's data.

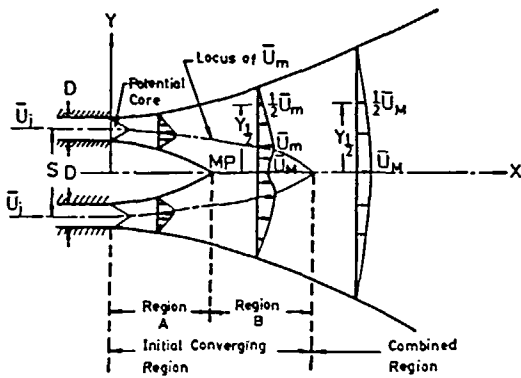


Figure 1 The flowfield of twin plane jets

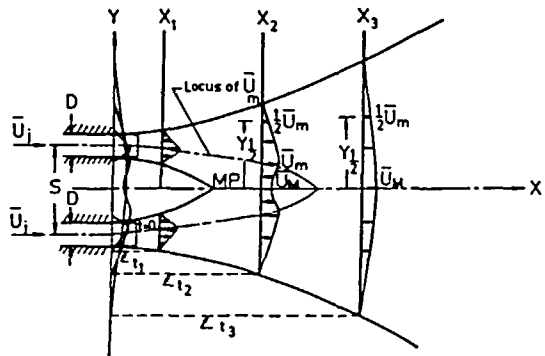
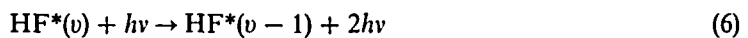
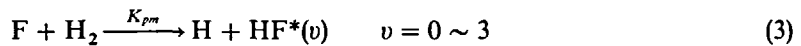


Figure 2 Simulation of twin jets instantaneous mixing to steady twin jets mixing: (a) instantaneous mixing mean velocity profiles observed at fixed x ; (b) mean velocity profile observed when moving with velocity \bar{U}_m

Chemical reacting and lasing action

In order to utilize the momentum solutions without chemical reaction, nitrogen gas is used as the diluent because it makes the density of main stream (fluorine atoms) almost the same as that of environment fluid (H_2). The assumption of chemical lasing reaction is one-step and one-direction. Under the above assumption, the chemical reaction equations of lasing flow involved are:



A pumping reaction is shown in (3), where m is one of e, f, g, h which is represented by the pumping reacting rate of energy level $v = 0, 1, 2, 3$ respectively. Equation (4) is a vibration-vibration collisional deactivation equation. Equation (5) is a vibration-translation collisional deactivation equation, where M is represented by $\text{N}_2, \text{H}_2, \text{H}$ and $\text{HF}^*(0)$, respectively. Equations (4) and (5) are the exchanged energy reactions which re-distribute the concentration of excited $\text{HF}^*(v)$ at different energy levels. Equation (6) is known as the lasing reaction or radiative deactivation.

Source conditions and constructed solution

The obtained Green's function of (1) by Hong²⁰ is considered to be the instantaneous point source solution of (1). In order to utilize the Green's function of (1) found by Hong²⁰ in constructing the PDF, in velocity space of fluid element, the source conditions have to be specified according to the given physical problem. Assume that for $t < t_0$, the two streams of twin jets are homogeneous and their PDF's distributions are Gaussian with respect to their own mean velocities (\bar{U}_j) and mean turbulent energies (E_{0j}). The ambient fluid is also assumed to be homogeneous and its PDF is Gaussian with respect to its own mean velocity (\bar{U}_∞) and turbulent energy (E_{01}).

Then the source conditions for the scalar C can be written as²:

$$S_{oi} = C_{i0} \cdot f_{oi}(\vec{u}_0) \tag{7}$$

where

$$\left\{ \begin{array}{l} f_{o1} = \frac{1}{(\frac{2}{3}\pi E_{o1})^{3/2}} \cdot \exp - \left[\frac{(u_0 - \bar{U}_\infty)^2 + v_0^2 + w_0^2}{\frac{2}{3}E_{o1}} \right] \\ \text{for } y \leq -(S + D)/2, -(S - D)/2 \leq y \leq (S - D)/2, y \geq (S + D)/2; x \leq 0 \\ f_{oi} = \frac{1}{(\frac{2}{3}\pi E_{oi})^{3/2}} \cdot \exp - \left[\frac{(u_0 - \bar{U}_i)^2 + v_0^2 + w_0^2}{\frac{2}{3}E_{oi}} \right] \quad i = 2, 3 \\ \text{for } -(S + D)/2 \leq y \leq -(S - D)/2, (S - D)/2 \leq y \leq (S + D)/2; x \leq 0 \end{array} \right. \tag{8}$$

According to the previous physical problem, the mass fraction source conditions of various species are:

$$\left\{ \begin{array}{l} C_{a0} = 0.66 \\ C_{d20} = 0.34 \quad \text{for } -(S + D)/2 \leq y \leq -(S - D)/2, (S - D)/2 \leq y \leq (S + D)/2; x \leq 0 \end{array} \right. \tag{10}$$

$$\left\{ \begin{array}{l} C_{b0} = 0.1 \\ C_{d10} = 0.9 \quad \text{for } y \leq -(S + D)/2, -(S - D)/2 \leq y \leq (S - D)/2, y \geq (S + D)/2; x \leq 0 \end{array} \right. \tag{11}$$

Dimensionless variables m and n are defined as:

$$\left\{ \begin{array}{l} m = (\hat{M}_p/\hat{M}_a)C_a \\ n = (\hat{M}_p/\hat{M}_b)C_b \end{array} \right. \tag{12}$$

According to (3), (10), (11), and (12), the source conditions m_0 and n_0 , for m and n respectively, become:

$$\left\{ \begin{array}{l} m_0 = \frac{21}{19} \times 0.66 \\ n_0 = 0 \quad \text{for } -(S + D)/2 \leq y \leq -(S - D)/2, (S - D)/2 \leq y \leq (S + D)/2; x \leq 0 \end{array} \right. \tag{13}$$

$$\left\{ \begin{array}{l} m_0 = 0 \\ n_0 = \frac{21}{2} \times 0.1 \quad \text{for } y \leq -(S + D)/2, -(S - D)/2 \leq y \leq (S - D)/2, y \geq (S + D)/2; x \leq 0 \end{array} \right. \tag{14}$$

According to the source conditions of (7)–(9), one can obtain the constructed PDF of twin jets flow as:

$$F = \int_{-\infty}^{+\infty} \int_{-\infty}^{+\infty} \int_{-\infty}^{+\infty} \int_{-\infty}^{+\infty} \int_{-\infty}^{+\infty} \left[\int_{-\infty}^{+\infty} G \cdot S_{o1} dy_0 - \int_{-(S+D)/2}^{-(S-D)/2} G \cdot S_{o1} dy_0 - \int_{(S-D)/2}^{(S+D)/2} G \cdot S_{o1} dy_0 + \int_{-(S+D)/2}^{-(S-D)/2} G \cdot S_{o2} dy_0 + \int_{(S-D)/2}^{(S+D)/2} G \cdot S_{o3} dy_0 \right] du_0 dv_0 dw_0 dx_0 dz_0 \tag{15}$$

The integration of (15) is very tedious¹. From the constructed PDF the ensemble average \bar{Q} or $\langle \bar{Q} \rangle$ can be obtained as:

$$\bar{Q} \text{ or } \langle \bar{Q} \rangle = \int_{-\infty}^{+\infty} F \cdot Q d\vec{u} \tag{16}$$

Let $Q = u_i' C_j$; then we can obtain the corresponding relation of turbulent correlations. In present problem the major mixing direction between fuel (H_2) and oxidant (F) is in y -direction, so (3) can be simplified, where the pumping reacting rate is assumed infinitely, i.e. $K_{pm} \rightarrow \infty$, as:

$$F_{m,v} \cdot F_{n,v} = 0 \tag{17}$$

where

$$\begin{cases} F_{m,v} = \int_{-\infty}^{+\infty} \int_{-\infty}^{+\infty} F_m(\vec{u}) \, du \, dv \\ F_{n,v} = \int_{-\infty}^{+\infty} \int_{-\infty}^{+\infty} F_n(\vec{u}) \, du \, dv \end{cases} \quad (18)$$

Under the assumption of the infinitely chemical reaction rate, the physical meaning of (17) is that the chemical reaction can occur only when fuel and oxidant simultaneously appear in the velocity cell. Equation (17) represents the *PDF* of species in velocity space which can be simplified to *v*-direction only, that is, the chemical reaction process can occur only when the fuel and oxidant coexist in *v*-velocity space. The *v*-direction velocity space is further divided into v_m and v_n , i.e.:

$$\begin{cases} (F_{m,v})_i \geq (F_{n,v})_i & \text{when } v = v_m \\ (F_{m,v})_i \leq (F_{n,v})_i & \text{when } v = v_n \end{cases} \quad (19)$$

where $(F_{m,v})_i$ and $(F_{n,v})_i$ are represented by $F_{m,v}$ and $F_{n,v}$, at no chemical reaction, respectively. Therefore (3), (17), and (19) can be replaced by:

$$\begin{cases} F_{m,v} = (F_{m,v})_i - (F_{n,v})_i \\ F_{n,v} = 0 \end{cases} \quad \text{when } v = v_m \quad (20)$$

$$\begin{cases} F_{n,v} = (F_{n,v})_i - (F_{m,v})_i \\ F_{m,v} = 0 \end{cases} \quad \text{when } v = v_n \quad (21)$$

Equations (20) and (21) are the final results for the present combustion model of twin jets with reaction flow. The species concentration with reacting can be calculated as:

$$\begin{cases} F_{a,v} = \frac{19}{21} F_{m,v} \\ F_{b,v} = \frac{2}{21} F_{n,v} \end{cases} \quad (22)$$

and,

$$\begin{cases} \langle C_a \rangle = \int_{-\infty}^{+\infty} F_{a,v} \, dv \\ \langle C_b \rangle = \int_{-\infty}^{+\infty} F_{b,v} \, dv \end{cases} \quad (23)$$

$$\begin{cases} \langle C_p \rangle = \int_{-\infty}^{+\infty} F_{p,v} \, dv \\ \langle C_c \rangle = \frac{1}{21} \langle C_p \rangle \\ \langle C_t \rangle = \frac{20}{21} \langle C_p \rangle \end{cases} \quad (24)$$

where C_t represents the total mass fraction of all excited energy level of $\text{HF}^*(v)$ after pumping reaction, i.e.:

$$\langle C_t \rangle = \langle C_e \rangle + \langle C_f \rangle + \langle C_g \rangle + \langle C_h \rangle \quad (25)$$

From the relation of pumping reaction rate between various excited $\text{HF}^*(v)$, then

$$\begin{cases} \langle C_e \rangle = \frac{1}{14} \langle C_t \rangle \\ \langle C_f \rangle = \frac{2}{14} \langle C_t \rangle \\ \langle C_g \rangle = \frac{10}{14} \langle C_t \rangle \\ \langle C_h \rangle = \frac{1}{14} \langle C_t \rangle \\ \langle C_d \rangle = 1 - \langle C_a \rangle - \langle C_b \rangle - \langle C_c \rangle - \langle C_e \rangle - \langle C_f \rangle - \langle C_g \rangle - \langle C_h \rangle \end{cases} \quad (26)$$

Processes of calculation

The Green's function is obtained by Hong²⁰ for the kinetic equations, the ensemble averages such as $\langle u_k \rangle$ and $\langle u'_k u'_k \rangle$ appearing in the equations are assumed to be known. The kinetic equation is linear and the solution of f is constructed via a linear summation of the weighted Green's functions according to the given source conditions. The, the ensemble averages $\langle u_k \rangle$ and $\langle u'_k u'_k \rangle$ are solved from (16) with $Q = u_k$ and $u'_k u'_k$. Therefore, an iterative scheme is needed to converge on the correct values for $\langle u_k \rangle$ and $\langle u'_k u'_k \rangle$. After $\langle u_k \rangle$ and $\langle u'_k u'_k \rangle$ are determined, all higher-order moments can be constructed from (16).

Calculation processes of chemical laser flow

The pumping reacting of chemical laser flow can proceed when the reactants are reached by molecular-wise mixing. The collisional deactivation quantities of various energy level between (x, η) and $(x + \Delta x, \eta)$, according to the chemical kinetic relations, can be written as:

$$\left\{ \begin{array}{l} \Delta\omega_{v-u}(0) = \frac{\rho}{\hat{M}_e} [K_{21} C_g(x, \eta) C_f(x, \eta) + K_{11} C_f^2(x, \eta)] \frac{\Delta x}{u} \end{array} \right. \quad (27)$$

$$\Delta\omega_{v-u}(1) = \frac{\rho}{\hat{M}_e} [K_{22} C_g^2(x, \eta) - K_{21} C_f(x, \eta) C_g(x, \eta) - C_f^2(x, \eta)] \frac{\Delta x}{u} \quad (28)$$

$$\Delta\omega_{v-u}(2) = \frac{\rho}{\hat{M}_e} [-K_{22} C_g^2(x, \eta) - K_{21} C_f(x, \eta) C_g(x, \eta) + K_{11} C_f^2(x, \eta)] \frac{\Delta x}{u} \quad (29)$$

$$\Delta\omega_{v-u}(3) = \frac{\rho}{\hat{M}_e} [K_{22} C_g^2(x, \eta) + K_{21} C_f(x, \eta) C_g(x, \eta)] \frac{\Delta x}{u} \quad (30)$$

$$\Delta\omega_{v-i}(0) = K_{a1} \frac{\rho}{\hat{M}_e} \left[\frac{\hat{M}_e}{\hat{M}_b} C_b(x, \eta) C_f(x, \eta) + \frac{\hat{M}_e}{\hat{M}_c} C_c(x, \eta) C_f(x, \eta) + C_e(x, \eta) C_f(x, \eta) \right] \frac{\Delta x}{u} \quad (31)$$

$$\Delta\omega_{v-i}(1) = K_{a2} \frac{\rho}{\hat{M}_e} \left[\frac{\hat{M}_e}{\hat{M}_b} C_b(x, \eta) C_g(x, \eta) + \frac{\hat{M}_e}{\hat{M}_c} C_c(x, \eta) C_g(x, \eta) + C_e(x, \eta) C_g(x, \eta) \right] \frac{\Delta x}{u} \quad (32)$$

$$\Delta\omega_{v-i}(2) = K_{a3} \frac{\rho}{\hat{M}_e} \left[\frac{\hat{M}_e}{\hat{M}_b} C_b(x, \eta) C_h(x, \eta) + \frac{\hat{M}_e}{\hat{M}_c} C_c(x, \eta) C_h(x, \eta) + C_e(x, \eta) C_h(x, \eta) \right] \frac{\Delta x}{u} \quad (33)$$

$$\left\{ \begin{array}{l} \Delta\omega_{cd}(0) = \Delta\omega_{v-u}(0) + \Delta\omega_{v-i}(0) \\ \Delta\omega_{cd}(1) = \Delta\omega_{v-u}(1) + \Delta\omega_{v-i}(1) - \Delta\omega_{v-i}(0) \\ \Delta\omega_{cd}(2) = \Delta\omega_{v-u}(2) + \Delta\omega_{v-i}(2) - \Delta\omega_{v-i}(1) \\ \Delta\omega_{cd}(3) = \Delta\omega_{v-u}(3) - \Delta\omega_{v-i}(2) \end{array} \right. \quad (34)$$

The $\chi_{\text{rad}}(v)$ is assumed as the P -branch instantaneous production rate of the radiative transitions at incident intensity $I_{v,j}^i$ from state $(v+1, j-1)$ to state (v, j) , where v and j are represented by the vibrational and rotational quantum numbers, respectively. Then the radiative transitions of $\Delta\chi_{\text{rad}}(v)$ between the adjacent two points can be written as:

$$\left\{ \begin{array}{l} \Delta\chi_{\text{rad}}(0) = \frac{\hat{M}_e}{\rho h N_A} \left[\frac{A_{0,6}}{v_{0,6}} (C_f(x, \eta) - \Lambda_{0,6} C_e(x, \eta)) \cdot I_{0,6}^i \right] \frac{\Delta x}{u} \\ \Delta\chi_{\text{rad}}(1) = \frac{\hat{M}_e}{\rho h N_A} \left[\frac{A_{1,5}}{v_{1,5}} (C_g(x, \eta) - \Lambda_{1,5} C_f(x, \eta)) \cdot I_{1,5}^i \right] \frac{\Delta x}{u} \\ \Delta\chi_{\text{rad}}(2) = \frac{\hat{M}_e}{\rho h N_A} \left[\frac{A_{2,4}}{v_{2,4}} (C_h(x, \eta) - \Lambda_{2,4} C_g(x, \eta)) \cdot I_{2,4}^i \right] \frac{\Delta x}{u} \end{array} \right. \quad (35)$$

Table 1 Gain parameters¹⁵

(a) Rotational-vibration energy

$$\begin{aligned}
 E(v,j) &= B_e j(j+1) - D_e j^2(j+1) + H_e j^3(j+1) - A_e j(j+1)(v+0.5) - \beta_e j^2(j+1)(v+0.5) \\
 D_e &= 4B_e^3/W_e^2 \\
 H_e &= 2D_e(12B_e^2 - A_e W_e)/3W_e^2 \\
 \beta_e &= D_e[(8W_e x_e/W_e) - 5(A_e/B_e) - (A_e^2 W_e/24B_e^3)]
 \end{aligned}$$

(b) Vibrational energy

$$G(v) = W_e(v+0.5) - W_e x_e(v+0.5)^2 + W_e y_e(v+0.5)^3 + W_e z_e(v+0.5)^4$$

(c) Transition frequency

$$v_{vj} = [E(v+1, j-1) + G(v+1) - E(v,j) - G(v)]C$$

(d) HF-system parameters

$$\begin{aligned}
 A_{v,j} &= \frac{8\pi^{5/2}}{3} \left(\frac{\ln 2N_A}{2\bar{M}_e K_b T} \right)^{1/2} \frac{\rho_j(R_v)^2}{hQ(v+1)} \cdot \exp \left[-\frac{E(v+1, j-1)}{K_b T} \right] \\
 \Lambda_{v,j} &= \frac{Q(v+1)}{Q(v)} \cdot \exp \left[\frac{E(v+1, j-1) - E(v,j)}{K_b T} \right] \\
 Q(v) &= \sum_{j=0}^{10} (2j+1) \cdot \exp \left[\frac{-E(v,j)}{K_b T} \right]
 \end{aligned}$$

(e) HF-system constants

$$\begin{aligned}
 A_e &= 0.796 \text{ cm}^{-1}, B_e = 20.95 \text{ cm}^{-1}, W_e = 4.14 \times 10^{-3} \text{ cm}^{-1} \\
 W_e x_e &= 90.0 \text{ cm}^{-1}, W_e y_e = 0.93 \text{ cm}^{-1}, W_e z_e = -0.014 \text{ cm}^{-1}
 \end{aligned}$$

(f) Relations of various chemical reaction rate

$$\begin{aligned}
 K_{p9} &= 10K_{pe} = 5K_{pf} = 10K_{ph} = K'_{pp} \cdot \exp(-E_A/RT) \\
 K_{22} &= 6K_{21} = 3K_{11} = K'_{22} T^{1.5} \\
 K_{a3} &= 3K_{a1} = 1.5K_{a2} = K'_{a3} T^{1.3}
 \end{aligned}$$

where

$$\begin{aligned}
 K'_{p9} &= 7 \times 10^{13} \text{ cm}^3 \text{ mole}^{-1} \text{ sec}^{-1} \\
 K'_{22} &= 6 \times 10^8 \text{ cm}^3 \text{ mole}^{-1} \text{ K}^{-1.5} \text{ sec}^{-1} \\
 K'_{a3} &= 3 \times 10^8 \text{ cm}^3 \text{ mole}^{-1} \text{ K}^{-1.3} \text{ sec}^{-1}
 \end{aligned}$$

where the parameters $A_{v,j}$, v_{vj} , and $\Lambda_{v,j}$ are listed in Table 1. And,

$$\begin{cases}
 \Delta\omega_{\text{rad}}(0) = \Delta\chi_{\text{rad}}(0) \\
 \Delta\omega_{\text{rad}}(1) = \Delta\chi_{\text{rad}}(1) - \Delta\chi_{\text{rad}}(0) \\
 \Delta\omega_{\text{rad}}(2) = \Delta\chi_{\text{rad}}(2) - \Delta\chi_{\text{rad}}(1) \\
 \Delta\omega_{\text{rad}}(3) = -\Delta\chi_{\text{rad}}(2)
 \end{cases} \quad (36)$$

The mass fraction of HF for various energy levels at location $(x + \Delta x, \eta)$ are:

$$\begin{cases}
 C_0(x + \Delta x, \eta) = \Delta\omega_p(0) + \Delta\omega_{cd}(0) + \Delta\omega_{\text{rad}}(0) + C_e(x, \eta) \\
 C_1(x + \Delta x, \eta) = \Delta\omega_p(1) + \Delta\omega_{cd}(1) + \Delta\omega_{\text{rad}}(1) + C_f(x, \eta) \\
 C_2(x + \Delta x, \eta) = \Delta\omega_p(2) + \Delta\omega_{cd}(2) + \Delta\omega_{\text{rad}}(2) + C_g(x, \eta) \\
 C_3(x + \Delta x, \eta) = \Delta\omega_p(3) + \Delta\omega_{cd}(3) + \Delta\omega_{\text{rad}}(3) + C_h(x, \eta)
 \end{cases} \quad (37)$$

where $\Delta\omega_p(v)$ are represented by the quantities of pumping reaction between (x, η) and $(x + \Delta x, \eta)$, and $C_v(x, \eta)$, are represented by the transported mass fraction from location (x, η) to $(x + \Delta x, \eta)$. Therefore the values of $\Delta\omega_p(v)$ at locations between $(x + \Delta x, \eta)$ and (x, η) are:

$$\begin{cases} \Delta\omega_p(0) = C_e(x + \Delta x, \eta) - C_e(x, \eta) \\ \Delta\omega_p(1) = C_f(x + \Delta x, \eta) - C_f(x, \eta) \\ \Delta\omega_p(2) = C_g(x + \Delta x, \eta) - C_g(x, \eta) \\ \Delta\omega_p(3) = C_h(x + \Delta x, \eta) - C_h(x, \eta) \end{cases} \quad (38)$$

According to the equation (37), $C_v(x + 2\Delta x, \eta)$ can be written as

$$C_v(x + 2\Delta x, \eta) = \Delta\omega_p(v) + \Delta\omega_{cd}(v) + \Delta\omega_{rad}(v) + C_v(x + \Delta x, \eta) \quad v = 0 \sim 3 \quad (39)$$

Calculations of chemical laser properties

(a) Local optical gain

$$\begin{cases} g_{0,6} = A_{0,6}[C_1(x, \eta) - \Lambda_{0,6}C_0(x, \eta)] \\ g_{1,5} = A_{1,5}[C_2(x, \eta) - \Lambda_{1,5}C_1(x, \eta)] \end{cases} \quad (40)$$

(b) Integrated gain

$$G_{vj} = \int_{-\infty}^{+\infty} g_{vj} dy \quad (41)$$

(c) Laser amplification

$$\frac{I_{vj}^i}{I_{vj}^0} = \exp(G_{vj}) \quad (42)$$

(d) Output power

$$\begin{aligned} P_{wr} &= \left[\int_0^{x_c} \sum_{v=0}^3 (I_{vj}^0 - I_{vj}^i) dx \right] z \\ &= \left[\int_0^{x_c} \sum_{v=0}^3 I_{vj}^i (\exp(G_{vj}) - 1) dx \right] z \end{aligned} \quad (43)$$

where x_c is the position of zero integrated gain, and x_c is called the laser optical cavity length.

(e) Chemical efficiency

$$\begin{aligned} \eta &= \frac{P_{wr}}{\Delta h} \quad (\Delta h = 31.6 \text{ Kcal/mole}) \\ &= \frac{P_{wr}}{4.18 \times 31600 \times \dot{n}_a} \end{aligned} \quad (44)$$

where Δh is the released energy of chemical equation (3), and \dot{n}_a is the mole concentration flow rate of fluorine atoms.

RESULTS AND DISCUSSION

In order to study the effects of twin plane jets HF chemical laser on turbulent energy, mass concentration of species, collisional deactivation Damkohler number, and radiative incident

intensity, the parameter of $\bar{S}(\equiv S/D)$ is fixed at 2. The velocity ratio of R is selected as 0 or 0.3 in order to study the effect of velocity ratio on the twin plane jets HF chemical laser flow.

PDF distributions of species

The PDF distributions of species at cross sections $x/D = 10$ along the y -axis are shown in Figures 3–6. At the centre line, the PDF distributions are symmetrized with $v' = 0$ axis because the flowfield is symmetric. At this time, the PDF distributions of fuel are shown in two sides of centre line. Along the y -axis upward for the same cross-section, the PDF distributions of fuel and oxidant are divided by three sections for $y/D = 1.0, 2.0$, as shown in Figures 4 and 5. For $y/D = 3.0$, the PDF distributions of fuel is small because it is almost pertinent to the edge of free stream, as shown in Figure 6.

Mass fraction distributions of species

The mass fraction distributions of reactants (F, H_2) and products (HF, H) at section $x/D = 10$ are shown in Figure 7. The feature of single jet type is still very obvious as shown in Figure 7. The maximum location of products is about at $y/D = 0.8 \sim 1.2$. The mass fraction distributions of HF for various energy levels at section $x/D = 10$ are shown in Figure 8 that is $HF(0) > HF(1) > HF(3) > HF(2)$. The lasing action of right jet of twin plane jets renders to the $HF(v)$ distributions have a concave profile at near $y/D = 1.0$. The mass concentration distributions of $HF(v)$ along the x -axis at $y/D = 0.6$ are shown in Figure 9. The energy level distributions of $HF(v)$ are total inversion at $x/D = 3.0 \sim 6.0$, i.e. $HF(2) > HF(1) > HF(0)$; and the $HF(v)$ energy levels distributions are partial inversion at $x/D = 6.0 \sim 9.0$, i.e. $HF(1) > HF(0), HF(1) > HF(2)$.

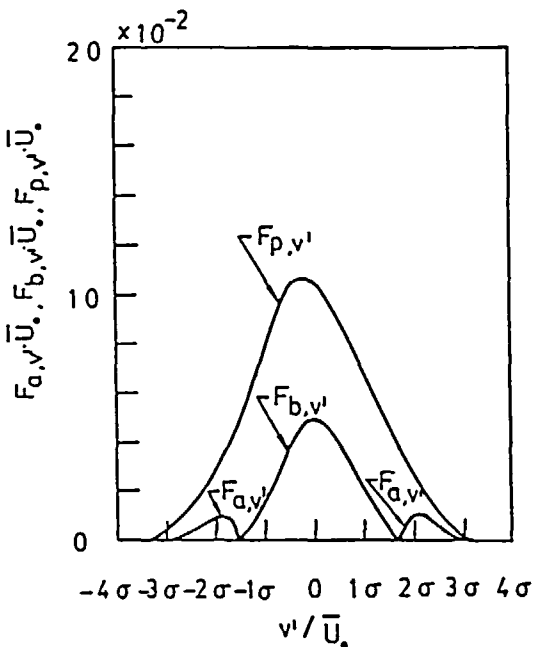


Figure 3 Species PDFs ($x/D = 10, y/D = 0$)

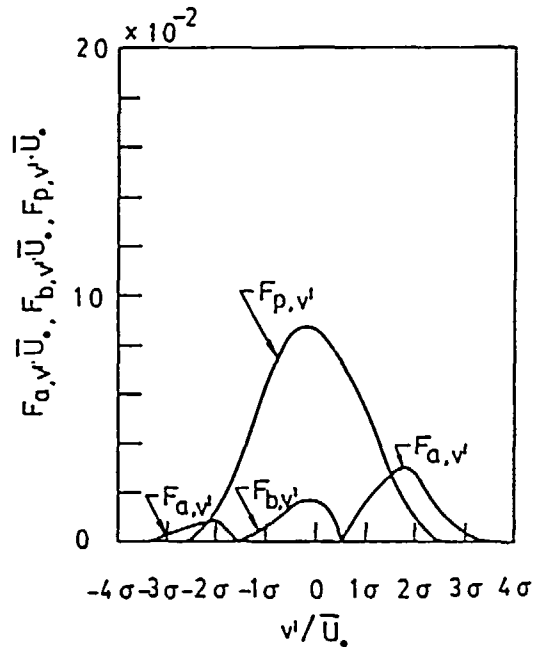


Figure 4 Species PDFs ($x/D = 10, y/D = 1.0$)

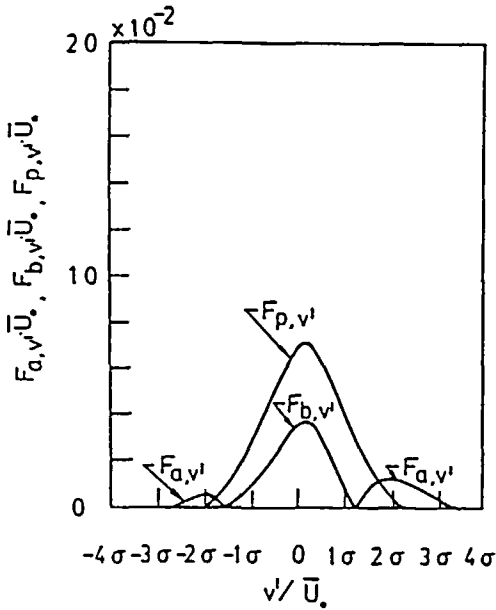


Figure 5 Species PDFs ($x/D = 10, y/D = 2.0$)

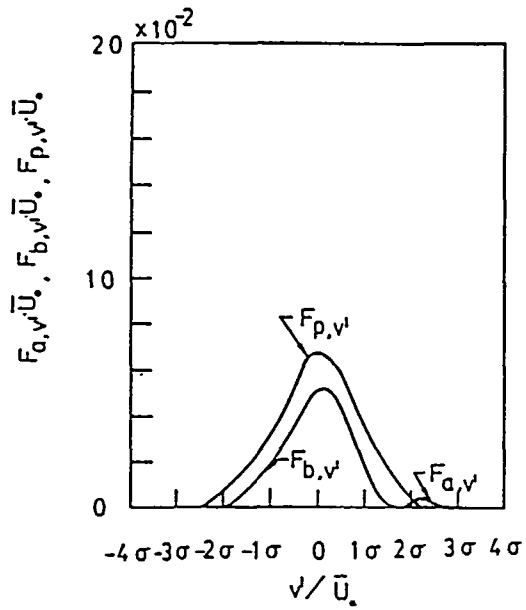


Figure 6 Species PDFs ($x/D = 10, y/D = 3.0$)

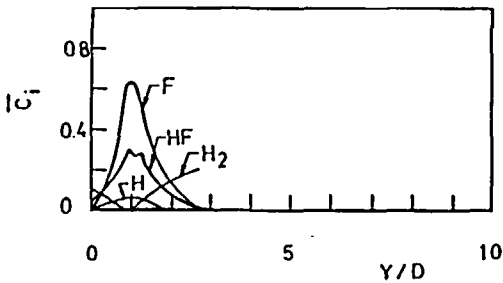


Figure 7 Mass fraction distributions of species ($x/D = 10$)

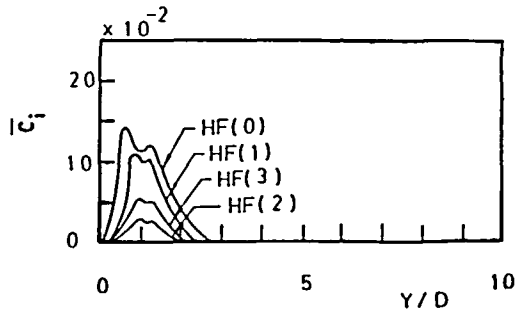


Figure 8 Mass fraction distributions of various excited HF(v) ($x/D = 10$)

Effect of turbulent energy of laser gain coefficients

The large velocity ratio R means that small velocity difference exist between main stream jet and surrounding fluid. The integrated gains of G_{15} and G_{06} distributions for $I_{15}^i = I_{06}^i = 0.3 \text{ kw/cm}^2$ are shown in Figure 10. Pumping reaction is faster proceeded at upstream when turbulent energy is increased ($R = 0.3$), and those integrated gains of G_{15} and G_{06} are also increased. The integrated gains of G_{15} at $x/D > 6.5$ and G_{06} at $x/D > 8.5$ are slightly decreased when the turbulent energy is increased ($R = 0.3$), and the affected action zone of laser also shrinks because the integrated gains are controlled by pumping and collisional reaction. The pumping reaction is a dominant factor at upstream; and the collisional reaction is a dominant factor at downstream due to the excited HF(v). The larger turbulent energy ($R = 0.3$) at downstream makes further to proceed the strong collisional reaction. The integrated gains decrease with the increased turbulent energy because the increased pumping reaction cannot compensate the losses of collisional reaction and radiative collisional at downstream.

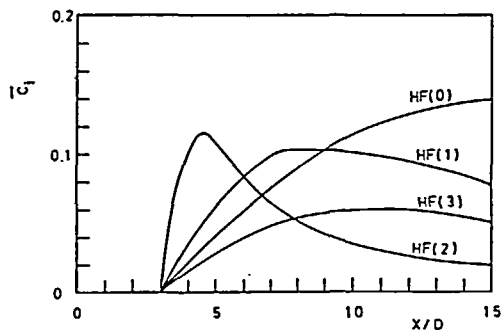


Figure 9 Mass fraction distributions of excited HF(v) (y/D = 0.6)

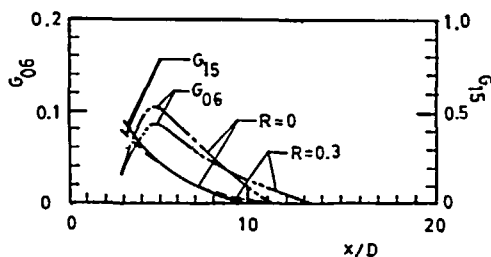


Figure 10 Effects of velocity ratios on integrated gain G_{06} and G_{15} ($I_{06}^i = I_{15}^i = 0.3 \text{ kW/cm}^2$, $C_{a0} = 0.66$, $C_{b0} = 0.05$)

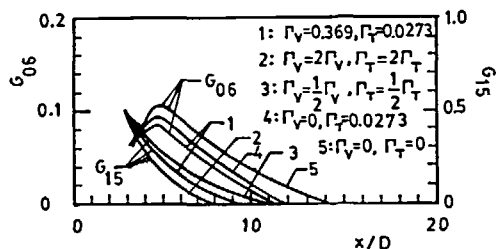


Figure 11 Collisional deactivation effects of $v-v$ and $v-t$ on integrated gain G_{06} and G_{15} ($I_{06}^i = I_{15}^i = 0.3 \text{ kW/cm}^2$, $C_{a0} = 0.66$, $C_{b0} = 0.10$)

Table 2 Effects of collisional reaction on the performance of chemical laser

	Γ_v	Γ_T	P_{wr} (W)
$R = 0$			
$C_{a0} = 0.66$	0.369	0.0273	2512
$C_{b0} = 0.10$	0	0.0273	2560
$I_{15}^i = I_{06}^i = 0.3 \text{ KW/cm}^2$	0	0	3070

Effect of collisional reaction on laser flow

Figure 11 and Table 2 show that the most of vibration-vibration collisional deactivative transform only the different energy levels. The vibration-translation collisional deactivation is a dominant factor for collisional deactivation of twin plane jets HF chemical laser flow.

Effect of radiative incident intensity on laser flow

The effect of radiative incident intensity on integrated gains are shown in Figure 12. The maximum value of G_{06} moves towards upstream when the incident intensity increase. The molecular of HF(2) is decreased and the molecular of HF(1) is increased in chemical laser flow which are resulted from the increasing I_{15}^i . The values of G_{06} are increased along with upstream

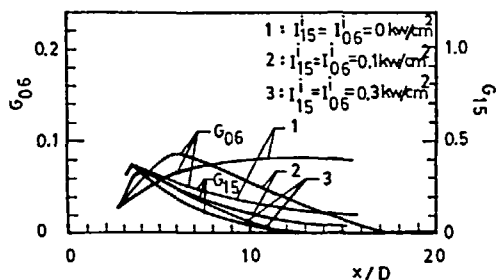


Figure 12 Effects of radiative incident intensity on integrated gain G_{06} and G_{15} ($C_{a0} = 0.66$, $C_{b0} = 0.10$)

Table 3 Effects of radiative incident on the performance of chemical laser

$I_{15}^i = I_{06}^i$ (KW/cm ²)	C_a	C_b	P_{wr} (W)	X_c (cm)
0.1	0.66	0.1	2490	6.6
0.3	0.66	0.1	2682	4.8
0.5	0.66	0.1	2913	3.7

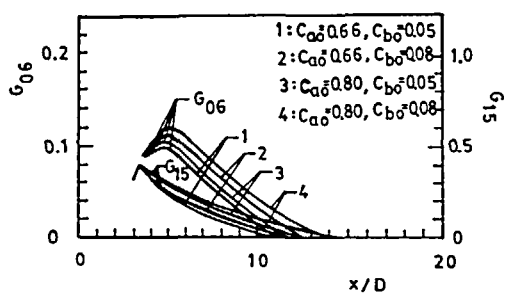


Figure 13 Effects of species concentration on integrated gain G_{06} and G_{15} ($I_{06}^i = I_{15}^i = 0.3 \text{ kw/cm}^2$)

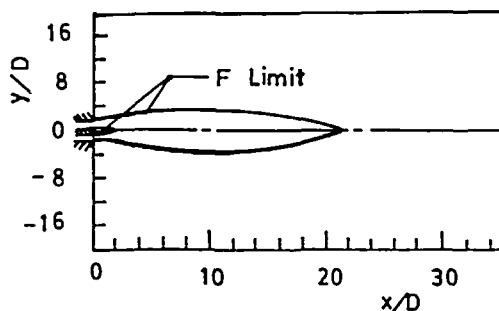


Figure 14 Flow structure of twin plane jets HF chemical laser

Table 4 Effects of reactive concentration on the performance of chemical laser

$R = 0$	C_a	C_b	\dot{n}_b/\dot{n}_a	\dot{n}_a (mole/sec)	X_c (cm)	P_{wr} (W)	η (%)
$I_{15}^i = 0.3 \text{ KW/cm}^2$	0.66	0.05	0.72	0.394	3.98	2914	5.72
	0.66	0.08	1.15	0.394	4.48	3067	6.10
$I_{06}^i = 0.3 \text{ KW/cm}^2$	0.80	0.05	0.59	0.478	5.28	3420	5.12
	0.80	0.08	0.95	0.478	5.70	3672	5.83

due to the cascade effect. The affected lasing zone is contracted, the loss of collisional deactivation is decreased, and the output power is increased when the optical cavity length is shorter, as shown in Table 3.

Effect of species concentration on laser flow

The effect of species concentration on the characteristics of chemical laser flow are shown in Figure 13 and Table 4. The more concentration of F would consume the more concentration of H_2 , therefore the loss of species concentration due to vibration-translation collision deactivation decreases. The values of G_{15} , G_{06} , and P_{wr} are increased with increasing F. The collisional loss of $HF(v) - HF(v)$ is promoted when pumping reaction is increased.

Flow structure of HF chemical laser

Flow structure of HF chemical laser is shown in Figure 14. The lasing reacting zone has been shown in Figure 14. The calculated results can provide an explanation for the existence of turbulent diffusion flame zone even under the infinitely fast pumping reaction rate.

CONCLUDING REMARKS

The study of twin plane jets chemical laser analysis is the fundamental of multiple plane jets chemical laser. The calculated results can provide to understand the inner structure of twin plane jets chemical laser. The chemical laser flow of twin plane jets is controlled by the dissipation rate under fast pumping reaction. The dissipation rate of turbulent flow is affected by the turbulent energy. The interaction of twin jets play an important role on the turbulent energy distribution. Hence the characteristics of chemical laser flow are directly influenced by the interaction of twin plane jets.

REFERENCES

- 1 Hong, Z. C. and Chuang, S. H. Kinetic theory approach to twin plane jets turbulent mixing analysis, *AIAA J.*, **26**, 303–310 (1988)
- 2 Chuang, S. H. and Hong, Z. C. Diffusion flame analysis of twin plane jets via a kinetic theory approach, *Int. J. Num. Meth. Fluids*, **13**, 341–354 (1991)
- 3 Chuang, S. H., Hong, Z. C. and Wang, J. H. Multiple-plane-jet turbulent mixing analysis via a kinetic theory approach, *Int. J. Num. Meth. Fluids*, **13**, 83–107 (1991)
- 4 Chuang, S. H. and Hong, Z. C. The multiple plane jets turbulent combustion analysis, *Trans. AASRC*, **18**, 1–12 (1985)
- 5 Chung, P. M. Turbulent chemically reacting flows, *Aerospace Cor. Techn. Rep. TR-1001(S2855-20)-5*, (1967)
- 6 Chung, P. M. A simplified statistical model of turbulent chemically reacting shear flows, *AIAA J.*, **7**, 1982–1991 (1969)
- 7 Polanyi, J. C. Proposal for an infrared laser dependent on vibrational excitation, *Chem. Phys. J.*, **34**, 347–348 (1961)
- 8 Kasper, J. V. V. and Pimentel, C. G. HCL chemical laser, *Phys. Rev. Lett.*, **14**, 352–354 (1965)
- 9 Kompa, K. L. and Pimentel, G. C. Hydrofluoric acid chemical laser, *Chem. Phys. J.*, **47**, 857 (1967)
- 10 Spencer, D. J., Jacobs, T. A., Mirels, H. and Gross, R. W. F. A continuous wave chemical laser, *Int. J. Chem. Kinet.*, **1**, 493 (1969)
- 11 Spencer, D. J., Mirels, H., Jacobs, T. A. and Gross, R. W. F. Preliminary performance of a CW chemical laser, *Appl. Phys. Lett.*, **16**, 235 (1970)
- 12 Spencer, D. J., Mirels, H. and Jacobs, T. A. Comparison of HF and DF continuous chemical laser: I. power, *Appl. Phys. Lett.*, **16**, 384 (1970); also Kwok, M. A., Giedt, R. R. and Gross, R. W. F. Comparison of HF and DF continuous chemical lasers: II. Spectroscopy, *Appl. Phys. Lett.*, **16**, 386 (1970)
- 13 Mirels, H. and Spencer, D. J. Power and efficiency of a continuous HF chemical laser, *IEEE J. Quant. Electron.*, **QE-7**, 501 (1971)
- 14 Cohen, N., Jacobs, T. A., Emanuel, G. and Wilkins, R. L. Chemical kinetic of hydrogen halide laser 1, The H_2-Cl_2 System, *Int. J. Chem. Kinet.*, **1**, 551 (1969)
- 15 King, W. S. and Mirels, H. Numerical study of diffusion-type chemical laser, *AIAA J.*, **10**, 1647 (1972)
- 16 Chung, P. M. and Shu, H. T. HF chemical laser amplification properties of an uniform, turbulent mixing laser, *Acta Astronaut.*, **1**, 385 (1974)
- 17 Kerber, R. L., Emanuel, G. and Whittier, J. S. Computer modeling and parametric study for a pulsed $H_2 + F_2$ laser, *Appl. Optics*, **11**, 1112 (1972)
- 18 Broadwell, J. E. Effect of exciting rate on HF chemical laser performance, *Appl. Optics*, **13**, 902 (1974)
- 19 Hong, Z. C. and Chen, L. HF chemical laser properties analysis in a turbulent plane jet, *CSME J.*, **5**, 45–66 (1984)
- 20 Hong, Z. C. Turbulent chemically reaction flows according to a kinetic theory, *Ph D Thesis*, Univ. of Illinois at Chicago (1975)